

Bar pattern speed at $z \sim 1 - 2$ to explore challenges of the Standard Cosmology

Virginia Cuomo¹ , Mahmood Roshan², J. Alfonso L. Aguerri^{3,4}
and Lorenzo Morelli¹

¹Instituto de Astronomía y Ciencias Planetarias, Universidad de Atacama,
Avenida Copayapu 485, Copiapó, Atacama 1530000, Chile
email: virginia.cuomo@uda.cl

²Department of Physics, Faculty of Science, Ferdowsi University of Mashhad,
P.O. Box 1436, Mashhad, Iran

³Instituto de Astrofísica de Canarias, calle Vía Láctea s/n, 38205 La Laguna, Tenerife, Spain

⁴Departamento de Astrofísica, Universidad de La Laguna,
Avenida Astrofísico Francisco Sánchez s/n, 38206 La Laguna, Tenerife, Spain

Abstract. Stellar bars drive the galaxy secular evolution. While rotating around the galaxy centre with a given angular frequency, the bar pattern speed, they sweep material and modify the galaxy structure. In the LCDM model, bars are expected to slow down by exchanging angular momentum with the other components and/or through dynamical friction exerted by the dark matter halo. The only direct method to derive the bar pattern speed, the Tremaine-Weinberg method, revealed that real bars rotate fast, stressing a tension between the observations, conducted to date in the local universe, and the LCDM model. Measuring the bar pattern speed to bars up to $z \sim 1 - 2$ will reveal if the expected bar evolutionary path is actually taking place and/or to confirm if the dark matter is able to exert friction. Using high resolution N-body simulations we tested the applicability of the Tremaine-Weinberg method to deep spectroscopy of the NIRSpec@JWST for a sample of bars at $z \sim 1 - 2$. Our analysis can be used to prepare an observational proposal to get dedicated data.

Keywords. galaxies: evolution, galaxies: general, galaxies: structure, dark matter

1. Bars and their properties across cosmic time

Stellar bars are observed in most of galactic discs in the nearby Universe, including the Milky Way (Erwin 2018). Stars in a bar mainly follow elongated orbits (Contopoulos 1981), while the bar itself rotates as a solid body around the galaxy centre.

A bar is described by its length (R_{bar} , the extent of the supporting orbits), strength (S_{bar} , the amplitude of the bar force), and pattern speed (Ω_{bar} , the angular frequency of its rotation around the galaxy centre). These properties define the bar rotation rate $\mathcal{R} = \Omega_{\text{bar}} / (R_{\text{bar}} V_{\text{circ}}) = R_{\text{cr}} / R_{\text{bar}}$, where V_{circ} is the galaxy circular velocity and R_{cr} is the bar corotation resonance. A bar can be fast, if $1.0 \leq \mathcal{R} \leq 1.4$, or slow if $\mathcal{R} < 1.4$ (Athanasoula 1992).

Bars drive the secular evolution of galaxies. Simulations show that as bars exchange angular momentum, R_{bar} and S_{bar} increase and Ω_{bar} decreases (Athanasoula 2013). Thus, gas is redistributed in the centre, forming complex structures, while the star formation rate can be enhanced/depleted (James 2016).

Understanding the role of bars requires studying their properties across time. Using data from the James Webb Space Telescope (JWST) with NIRCam, recently Guo (2022)

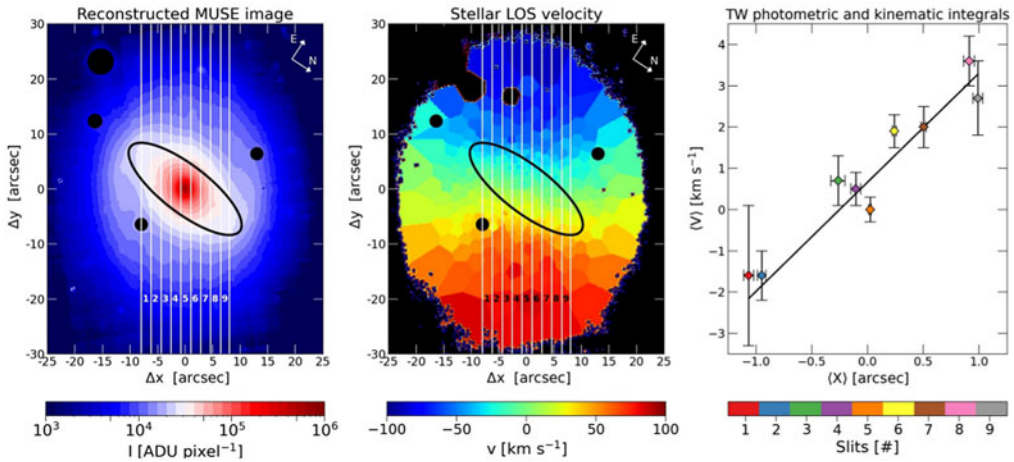


Figure 1. TW analysis of NGC 4277 on MUSE data. Left: MUSE image with the slits (white) and the bar (black). Centre: stellar LOS velocity map. Right: kinematic (V) vs. photometric (X) integrals and their best fit (solid line), giving $\Omega_{\text{bar}} = 24.7 \pm 3.4 \text{ km kpc}^{-1} \text{ s}^{-1}$. From Buttitta (2022).

discovered six barred galaxies at $z > 1$, including the two highest redshift bars known so far ($z \sim 2.14$ and 2.31). This means that bars are present in galaxies since ancient epochs. However, no advanced studies of these objects is available, requiring further investigation.

Theoretical studies in the LCDM framework show that a massive and centrally-concentrated DM halo slows down the bar exerting dynamical friction. Fast bars should be embedded in DM halos with a low central density (Debattista 2000), rare according to the LCDM model. Measuring \mathcal{R} is crucial to confirm the bar slowing down and it requires both R_{bar} and Ω_{bar} . While images are used to get R_{bar} , Ω_{bar} requires kinematic measurements as well. The only model-independent method to get Ω_{bar} is by Tremaine & Weinberg (1984, TW). It requires the stellar surface density from photometry and the line-of-sight (LOS) velocity from spectra to define the luminosity-weighted position and LOS velocity (the photometric (X) and kinematic (V) integrals, respectively) along slits aligned with the disc major axis. The linear relation between the integrals gives Ω_{bar} (Fig. 1). Thank to integral-field spectroscopy, a large number of galaxies have been analysed to date, but up to $z \sim 0.1$, making it impossible to discuss bar evolution across time.

Most of the analysed bars are fast: the expected bar slowing down was not observed in nearby galaxies (Cuomo 2020). If it would take place, bars at $z > 1$ should rotate even faster. Analysing hydro-dynamical simulations in the LCDM context from IllustrisTNG and EAGLE, Roshan (2021) confirmed the bars' slowing down, feeding the tension between the LCDM model and observations (Fig. 2). This failure is added to other documented issues of the LCDM cosmology (Kroupa 2012), with implications for our understanding of gravity. Given the fast bar-tension is based on Ω_{bar} measurements at $z < 0.1$, to understand whether the expected bar slowing down has even taken place, it is necessary to measure Ω_{bar} and \mathcal{R} at the dawn of bar formation: we suggest to push the application of the TW method at $z > 1$, testing the applicability of the method for future NIRSpec@JWST observations.

2. Bar properties at $z \sim 1 - 2$: applicability of the TW method

To date, the TW method has been applied only at $z < 0.1$, given the analysis requires high quality data (in terms of spatial and spectral resolution), a suited

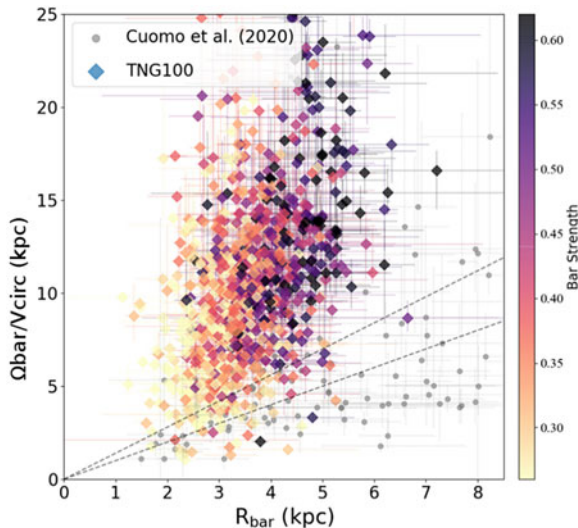


Figure 2. The bar rotation rate (given as the relation between $V_{\text{circ}}/\Omega_{\text{bar}}$ and R_{bar}) for galaxies from the IllustrisTNG simulation. The points are color-coded according to the value of S_{bar} . The solid grey circles represent the observational results from Cuomo (2020). The dashed lines mark the fast bar regime ($\mathcal{R} = 1.0 - 1.4$). A strong tension between the results from IllustrisTNG and observational studies is clear. From Roshan (2021).

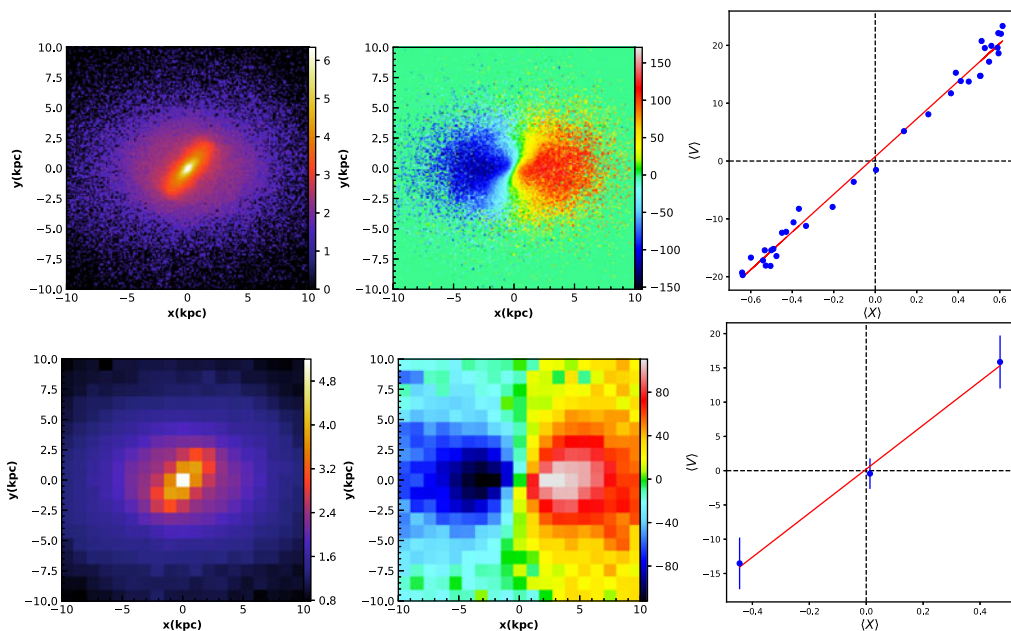


Figure 3. From left to right: surface density, LOS velocity, TW integrals, and the best-fit value of Ω_{bar} . In the first (second) row, we assume $201 \times 201 (19 \times 19)$ pixel² ($a_r \approx 0.1 (1.05)$ kpc).

wavelength and spatial coverage, and a careful sample selection. Here we demonstrate that TW measurements of Ω_{bar} at $z > 1$ are now possible due to the JWST instrumentation, using simulated data from IllustrisTNG, adapted to mimic NIRSpect@JWST observations.

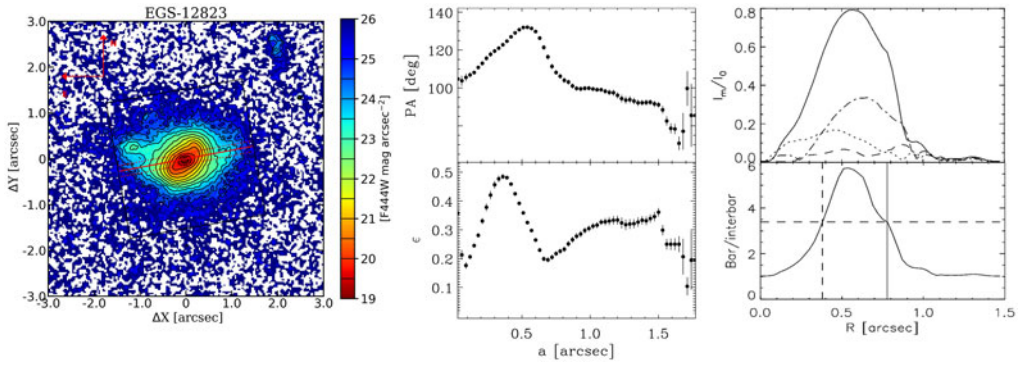


Figure 4. From left to right: JWST-F444W images of EGS-12823 with slits (red); radial profiles of PA and ellipticity, used to derive disc parameters (disc PA= 85° , $i47^\circ$); Fourier analysis: amplitudes of the first Fourier components, and bar/interbar intensity ratio, used to derive $R_{\text{bar}}=0.78$ arcsec and $S_{\text{bar}}=0.79$.

We adopt data from the IllustrisTNG50, providing the highest resolution within the Illustris project. We identify disc barred galaxies with similar properties as the sample of barred galaxies at $z \sim 1 - 2$ observed by Guo (2022), with stellar masses $M_* > 10^{10} M_\odot$, following Roshan (2021). We consider the subhalo with ID = 21 at $z = 1$. Indeed, this galaxy hosts a bar with $R_{\text{bar}}=6.8$ kpc with an intermediate orientation with respect to the disc axes. Moreover, we inclined the disc to have $i = 45^\circ$, to satisfy the requests of the TW method.

We derive the true $\Omega_{\text{bar}}=31.2 \pm 0.5 \text{ kpc}^{-1} \text{ s}^{-1}$, with velocity and position of each stellar particle, as Roshan (2021). We build the surface density and LOS kinematic maps of the stellar particles, assuming a given area per pixel a_r^2 . We define several slits crossing the bar and along the disc major axis to measure the integrals, using the signal from the 2D maps. We fit the integrals with a straight line, assuming $\sqrt{\bar{v}}/N$ to get the errors on (V) , where \bar{v} is the mean LOS velocity of each pixel and N is the number of the pixels. We build maps with $201 \times 201 \text{ pixel}^2$ (i.e. $a_r \approx 0.1$ kpc), and we find $\Omega_{\text{bar}}=32.6 \pm 0.1 \text{ kpc}^{-1} \text{ s}^{-1}$, compatible within 3σ with the true value (Fig. 4). We progressively degrade the spatial resolution by increasing a_r (i.e. decreasing the number of pixels). This is equivalent to shifting the galaxy at higher z . The number of definable slits progressively decreases while the error on Ω_{bar} increases. Assuming maps with $19 \times 19 \text{ pixel}^2$ (i.e. $a_r \approx 1.1$ kpc) we could define three slits (the minimum number) and derive $\Omega_{\text{bar}}=30.8_{-5.9}^{+6.0} \text{ kpc}^{-1} \text{ s}^{-1}$. This is compatible with the true value (but with a larger error, Fig. 4). Given with NIRSspec@JWST data a spatial resolution of is < 1.3 kpc at $z \sim 1$ is reachable, we conclude that the TW method is applicable using those kind of data.

3. Future perspectives and conclusions

We tested the applicability of the TW method for bars at the dawn of bar formation: this is needed to study Ω_{bar} and \mathcal{R} across cosmic time to understand whether the bar slowing down predicted by the LCDM model has even took place.

In particular, we used simulated data from IllustrisTNG with similar characteristics as the bars at $z \sim 1 - 2$ observed by Guo (2022), mimicking NIRSspec@JWST observations. We showed that the TW method can be applied at ancient cosmic time.

The application of the TW method requires a careful photometric analysis to identify the suited target, derive the disc properties to fine-tune the definition of the slits along which to measure the integrals, and measure the photometric bar properties, (i.e. R_{bar})

to derive \mathcal{R} . In Fig. 4 we show a preliminary analysis for EGS-12823, suited for the TW analysis.

The applicability study of the TW method presented here can be used to prepare an observational proposal to get dedicated NIRSpc@JWST in the future.

References

- Athanassoula 1992, MNRAS, 259, 345
Athanassoula, Machado, Rodionov 2013, MNRAS, 429, 1949
Buttitta et al. 2022, A&A, 664, L10
Contopoulos 1981, A&A, 102, 265
Cuomo et al. 2020, A&A, 641, A111
Debattista & Sellwood 2000, ApJ, 543, 704
Erwin 2018, MNRAS, 474, 5372
Guo et al. 2022, arXiv e-prints, arXiv:2210.08658
James & Percival 2016, MNRAS, 457, 917
Kroupa 2012, PASA, 29, 395
Roshan et al. 2021, MNRAS, 508, 926
Tremaine & Weinberg 1984, ApJ, 282, L5